ON THE ELECTROCHEMICAL BEHAVIOR OF SOME SELENINYL AZULENE COMPOUNDS

Alexandra OPRISANU[1], Georgiana Anca INEL[2], Eleonora-Mihaela UNGUREANU[3*], Liviu BIRZAN[4*]

This work is devoted to the electrochemical characterization of two seleninyl azulene compounds. The investigations were performed by cyclic voltammetry and differential pulse voltammetry. The redox processes for each compound were established, analyzed and assessed to the particular processes which can take place during oxidation and reduction scans. This assessment was based on the similarity of the two seleninyl compounds structure connected to the number of substituents.

Keywords: seleninyl azulene compounds, cyclic voltammetry, differential pulse voltammetry

1. Introduction

Due to the involvement of selenium in the metabolic cycle of living organisms [1, 2] and its presence in some organic molecules, the interest for the electrochemistry of organoselenium compounds is increasing, also caused by the interest from pharmaceutical point of view [3, 4]. The study of electrochemical behaviour of organic selenides aims to clarify the understanding of their redox processes in biological systems [3, 5].

The electrochemical study of some organoselenium compounds [6–15], such as 1-(phenylseleninyl)azulene and 1,3-bis(phenylseleninyl)azulene has shown that aromatic selenides are more stable toward electrochemical reduction, compared to alkylselenides, because the aryl radicals have a higher electron density than alkyl radicals and they are generated difficult from anion radicals [16-18].

In this paper, the electrochemical behavior of 1-(phenylseleninyl)azulene (compound **1**) and 1,3-bis(phenylseleninyl)azulene (compound **2**) has been

[1]Faculty of Applied Chemistry and Material Sciences, University POLITEHNICA of Bucharest, Romania
[2] Faculty of Applied Chemistry and Material Sciences, University POLITEHNICA of Bucharest, Romania
[3] Faculty of Applied Chemistry and Material Sciences, University POLITEHNICA of Bucharest, Romania, *correspondent author, e-mail: em_ungureanu2000@yahoo.com,
[4] Institute of Organic Chemistry "C.D. Nenitzescu" of Romanian Academy, Bucharest, Romania, *correspondent author, e-mail: lbirzan@yahoo.com

studied on a stationary electrode in acetonitrile containing tetra-butyl-ammonium perchlorate as supporting electrolyte salt. The new seleninyl azulene compounds (**1** and **2**) have similar structures (Fig. 1), with one or two phenylseleninyl substituents on the 5 membered ring of the azulene skeleton. Studies have been performed on a glassy carbon electrode [19], in order to elucidate the electrode reactions electrochemical. These data were examined in the light of influence of the number and effect of phenylseleninyl substituents. The peak potential values and, therefore, the order in reduction or oxidation processes of compounds **1**, **2** help us to predict the properties of similar compounds in the same class. A detailed analysis of the peaks shapes and heights could bring information about the redox behavior of these compounds. The electrochemical characterization is useful to select the best polymerization conditions for each ligand in order to obtain chemically modified electrodes. In the same time, their study confirms that azulene moiety is a peculiar aromatic system with high electrochemical reactivity, thus allowing an evidence of more subtle interactions involving compounds with very similar structures [19].

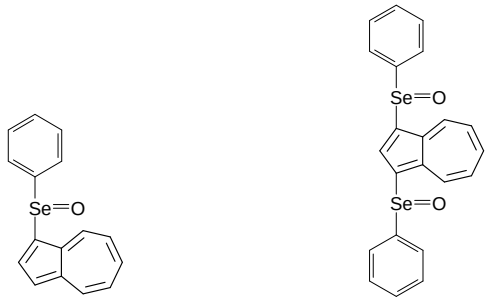

1 2

Fig.1. Structures of investigated compounds **1** and **2**

2. Experimental

Seleninyl azulene derivatives **1** and **2** have been prepared by chemical oxidation with sodium periodate of the corresponding selanyl derivatives [1]. Acetonitrile (CH_3CN) and tetrabutylammonium perchlorate (TBAP) from F1uka were used as received for electrochemical study, as solvent and supporting electrolyte salt, respectively.

The electrochemical experiments were carried out using a PGSTAT 12 AUTOLAB potentiostat in a three-electrode cell. The working electrode was a Metrohm glassy carbon disk (having the diameter of 3 mm). The active surface was polished before each experiment with diamond paste (2 μm) and cleaned with the solvent. Ag/10 mM $AgNO_3$ dissolved in 0.1 M TBAP, CH_3CN was used as reference electrode. The electrode potential was finally referred to the potential of

the ferrocene/ferricinium redox couple (Fc/Fc^+) which in our experimental conditions was +0.07 V. A platinum wire was used as auxiliary electrode. The experiments were performed at room temperature under argon atmosphere by cyclic voltammetry (CV) and differential pulse voltammetry (DPV). The CV curves were generally recorded at 0.1 Vs^{-1} scan rate, or at various scan rates (0.1 - 1 Vs^{-1}) - when studying the influence of this parameter. DPV curves were recorded at 0.01 Vs^{-1} with a pulse height of 0.025 V and a step time of 0.2 s.

3. Results and Discussion

Each anodic and cathodic CV and DPV curves has been recorded starting from the stationary potential for various concentrations (0 – 2 mM) of each of the investigated compounds in 0.1 M TBAP solutions in acetonitrile. The data from cyclic voltammetry experiments enables the determination of the reversible (r), quasireversible (q) and irreversible (i) character of each process, and from DPV, the number of processes and the potentials at which the process rate has a maximum value (peak potential).

Study of **1**

The DPV curves obtained for different concentrations of **1** are presented in Fig. 2. Four anodic (a1 – a4) and two main cathodic (c1 – c2) processes are observed, denoted in the order at which they appear in the differential-pulse voltammograms. A series of corresponding CV curves for increasing concentrations of **1** are shown in Fig. 2, below the DPV curves. The CV oxidation and reduction processes are denoted in connection with the DPV peaks, in agreement with their peak potentials given in Table 1. The dependencies of anodic and cathodic peaks currents on concentration of **1** have been evaluated and are shown in Fig. 3. They are linear; their slopes are given in Table 2. The equations of the dependencies of peaks potential on logarithm of concentration for anodic and cathodic processes are specified in Table 2. The cathodic peaks are situated at constant potentials, while the anodic ones vary with 33 mV/decade (for a1), 17 mV/decade (for a2) and 50 mV/decade (for a3).

The influences of the potential scan rate and scan range on the CV curves have also been examined; the curves for the concentration of 2 mM are presented in Fig. 4. The data from Fig. 2 and 3 gives the possibility to estimate the character of each peak (Table 1). The diffusion coefficient of **1** at room temperature for its oxidation process has been calculated from the slope of peak a1 *vs* the square root of the scan rate, using Randles-Sevcik equation for two electrons transferred: $D_1 = 1.08 \cdot 10^{-6}$ cm^2/s.

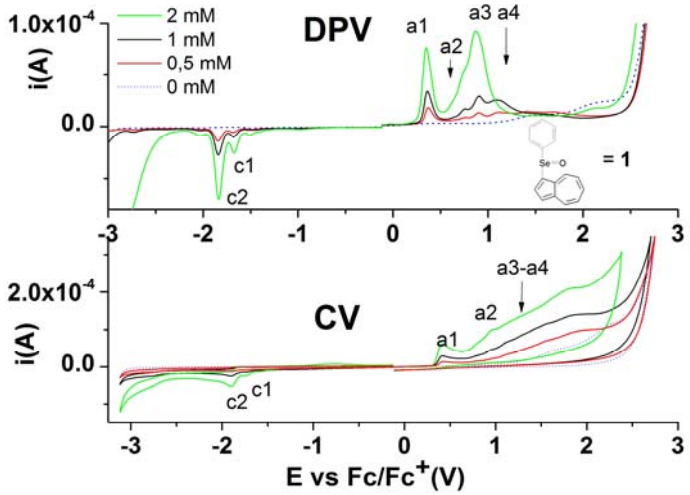

Fig. 2. DPV and CV curves (0.1 V/s scan rate) for different concentrations of 1 in 0.1M TBAP, CH_3CN on glassy carbon disk (3mm diameter)

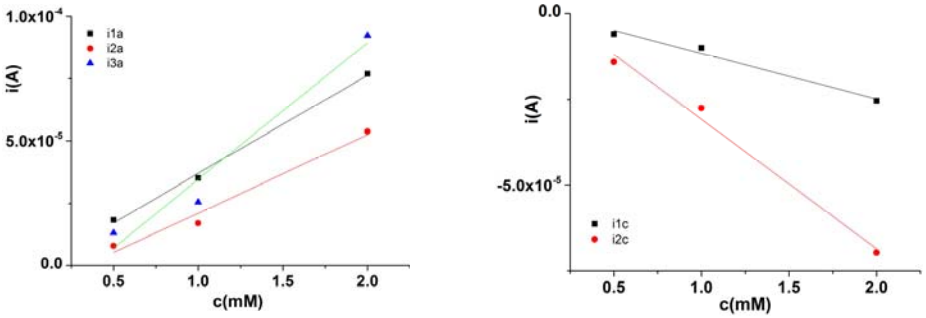

Fig. 3. Dependencies of the anodic peak currents ia1, ia2, ia3 and cathodic (ic1, ic2) on concentration of **1** (c) from DPV experiments

Table 1

Potentials (V) of the peaks for 1 at [1] = 1mM and their assessment

Symbol of the peak	Technique		Assesment
	DPV	CV(0,1V/s)	
a1	0.37	0.41 (i, EC)	Dication formation
a2	0.76	**(i)	Oxidation of dication stabilization products
a3	0.90	**(i)	Oxidation of dication stabilization products
a4	1.12	**(i)	Oxidation of dication stabilization products
c1	-1.67	-1.73 (r/q) *	AzSe(O)Ph -> AzSePh
c2	-1.84	-1.89 (i) *	AzPhSe reduction

*r - reversible process; q - quasi-reversible process; i - irreversible process.
** shoulder

Table 2

Equations of peak current (i_p, A) and peak potential (E_p, V) dependencies on concentration (c, mM) of 1

Peak	i_p *vs* c	E_p *vs* c
a1	$i = -2.5\cdot10^{-6} + 3.94\cdot10^{-5}\cdot c$	$E = 0.36 - 0.033\cdot\log c$
a2	$i = -10.23\cdot10^{-6} + 3.136\cdot10^{-5}\cdot c$	$E = 0.76 - 0.017\cdot\log c$
a3	$i = -20.24\cdot10^{-6} + 5.482\cdot10^{-5}\cdot c$	$E = 0.89 - 0.05\cdot\log c$
c1	$i = 1.71\cdot10^{-6} - 1.33\cdot10^{-5}\cdot c$	E = -1.67
c2	$i = 6.95\cdot10^{-6} - 3.77\cdot10^{-5}\cdot c$	E = -1.84

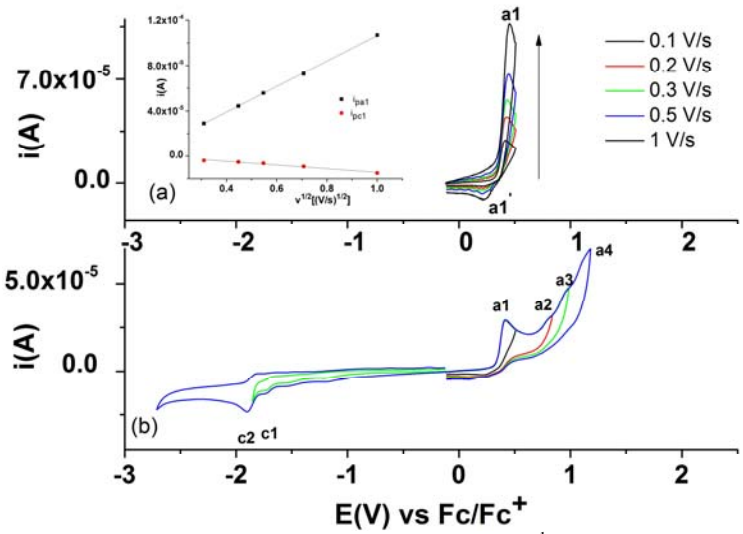

Fig. 4. CV curves at different scan rates: 0.1; 0.2; 0.3; 0.5; 1 Vs^{-1} in the domains of the peaks c1 and a1, respectively(a) and at various scan domains at 0.1 Vs^{-1} (b) for **1** (2 mM) in 0.1M TBAP, CH_3CN ;(inset of (a) peak currents dependencies on the square root of the scan rate)

An explanation of the electrochemical behavior of these compounds can be seen in Scheme 1. It is based on the fact that azulene is a very easily oxidizable moiety, and it relatively easy forms tropylium like structure radical cations ($M^{+\cdot}$). These intermediates either disproportionate or are further oxidized to a dication (M^{2+}), which interacts easily with another molecule to form dimeric (D) species. Anyway, two electrons per azulene moiety are removed (a process characterized by the peak a1) to obtain double ionized dimeric species. Due to the low energy bonding between carbon and selenium atoms, the phenylseleninyl group can be removed relatively easy as cationic species, with the formation of phenylseleninic acid. Therefore, the generated radical cations can attack the dimer forming superior oligomers (trimers, T, tetramers, Q). These oligomers can eliminate protons or phenylseleninyl cations to generate a polymeric structure, which is

further oxidized at the anode. The facile elimination of the chalcogenic functional groups caused by the weak C-X bond was proved in similar cases by the *ipso* substitution of RS group, for example by formyl [20]. Therefore, the upper oxidation potentials are almost the same for all chalcogens, due to their massive elimination during the polymerization processes. The oxidation potentials are higher than those observed for the monomers (the neutral oligomers should oxidize faster than the monomers), because some positive charges are present in these oligomers. The azulenic oligomers are known to loose electrons [21], but the most stable ones contain only a positive charge for several azulene moieties. Another radical cation of the starting material can interact to generate a charged tetramer, which is also stabilized by elimination of proton and $PhSe(O)^+$ species. Azulene moiety is able to form small oligomers and, subsequently, the polymerization process does not advance too much. In the presence of water, at higher potentials, some quinonic structures are generated by water addition to dicationic azulene moieties. Finally, the azulene frame is modified by transpositions with the generation of numerous products that are responsible for the envelope of peaks which are present at higher positive potentials. Their structures are similar to those resulted by chemical oxidation with oxygen [22], or even bromine [23].

The cathode processes consist in *i)* the reduction of selenium atom from Se(IV) to Se(II) (process characterized by the peak c1), and *ii)* reduction of the formed AzSe(II)Ph to a radical anion intermediate, and finally, to the dianion, which splits after protonation to azulene and $PhSe^-$ (seen as peak c2).

It can be noticed that the concentration dependencies of the anodic peak currents are different for the first two peaks a1 and a2, which vary with about 3.5 $\mu A(mM)^{-1}$. The third anodic peak, a3, has a slope of about 5.5 $\mu A(mM)^{-1}$. For the cathodic peaks, the dependency of current on concentration is different, the peak c1 has a slope of -14.3 $\mu A(mM)^{-1}$, and the second peak c2 increases in absolute value, reaching a bigger slope of -38.4 $\mu A(mM)^{-1}$. These dependencies are useful from analytical point of view and can be used to build calibration curves for the evaluation of **1** concentrations using DPV curves.

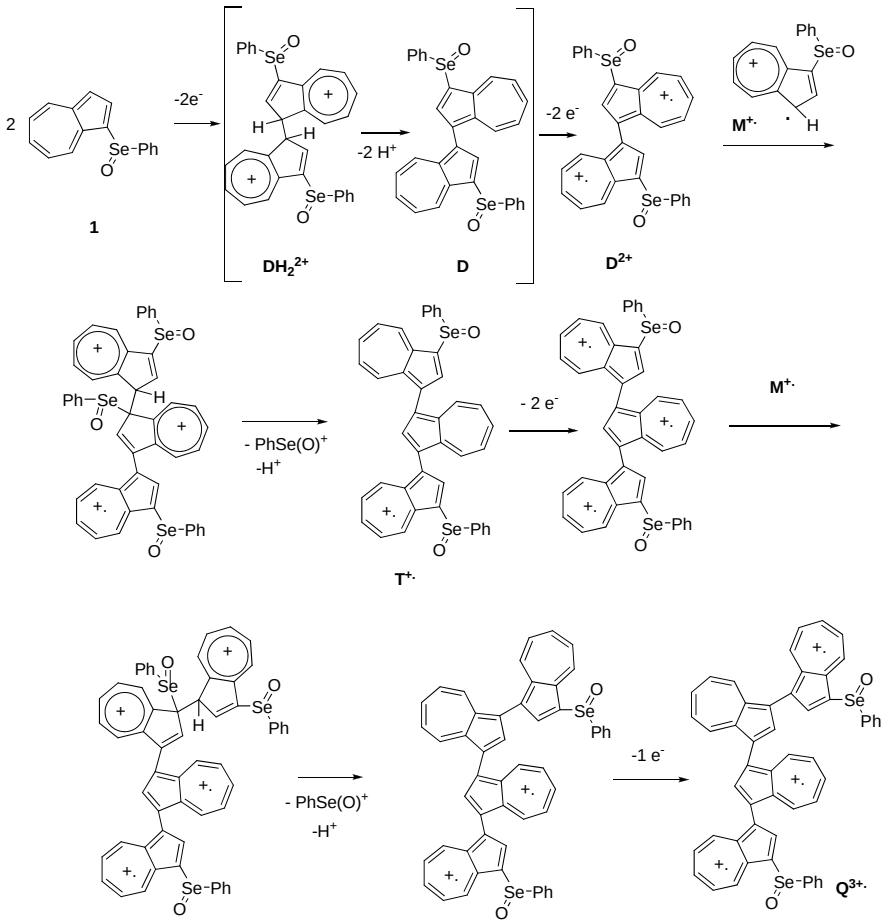

Scheme 1

Study of **2**

The DPV curves obtained for different concentrations of **2** are presented in Fig. 5. Five anodic (a1 – a5) and two close cathodic (c1-c2) processes are observed, denoted in the order in which they appear in the differential pulse voltammograms. The CV curves for increasing concentrations of **2** are also shown in Fig. 5, bellow the DPV curves.

The influences of the potential range of scanning and scan rate on the CV curves are presented in Fig. 7. The data from Figs. 5 and 6 enables establishing the character of each peak according to reversibility criteria (Table 3).

The diffusion coefficient of **2** during its oxidation has been estimated from the slope of the peak a1 *vs* square root of the scan rate, using Randles-Sevcik equation for two electrons transferred: $D_2 = 3.05 \cdot 10^{-6}$ cm^2/s.

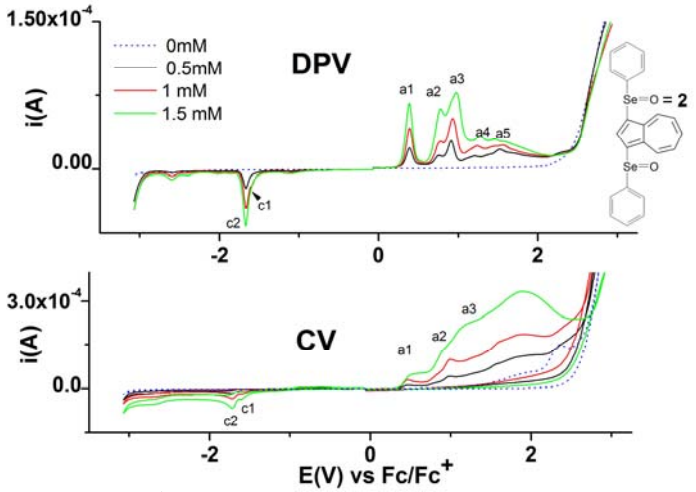

Fig 5. DPV and CV (0.1 Vs^{-1} scan rate) curves for different concentrations of **2** in 0.1M TBAP, CH_3CN, on glassy carbon disk (3 mm in diameter) electrode

Table 3

Potentials (V) of the peaks for 2 at [2] = 1mM and their assessment

Symbol of the peak	Technique		Assessment
	DPV	CV	
a1	0.39	0.46 (i)	Dication formation
a2	0.77	**	Oxidation of dication stabilization products
a3	0.93	**	Oxidation of dication stabilization products
a4	1.24	**	Oxidation of dication stabilization products
a5	1.56	**	Oxidation of dication stabilization products
c1	-1.61	**	$Az[Se(O)Ph]_2$ -> $Az(SePh)_2$
c2	-1.67	-1.72 (r/q) *	AzPhSe reduction

*r – reversible process; q – quasi-reversible process; i – irreversible process;** shoulder

Table 4

Equations of peak current (i_p, A) and peak potential (E_p, V) dependencies on concentration (c, mM) of 2

Peak	i_p *vs* c	E_p *vs* log c
a1	$i = 14.57 \cdot 10^{-6} + 2.03 \cdot 10^{-5} \cdot c$	$E = 0.39 + 0.004 \cdot \log c$
a2	$i = 8.93 \cdot 10^{-6} + 1.42 \cdot 10^{-5} \cdot c$	$E = 0.76 + 0.048 \cdot \log c$
a3	$i = 21.15 \cdot 10^{-6} + 2.28 \cdot 10^{-5} \cdot c$	$E = 0.93 + 0.043 \cdot \log c$
a4	$i = 9.98 \cdot 10^{-6} + 1.02 \cdot 10^{-5} \cdot c$	$E = 1.23 + 0.077 \cdot \log c$
a5	$i = 18.64 \cdot 10^{-6} + 0.43 \cdot 10^{-5} \cdot c$	$E = 1.55 + 0.093 \cdot \log c$
c1	$i = 1.23 \cdot 10^{-6} - 1.43 \cdot 10^{-5} \cdot c$	$E = -1.61$
c2	$i = -0.61 \cdot 10^{-6} - 3.84 \cdot 10^{-5} \cdot c$	$E = -1.67$

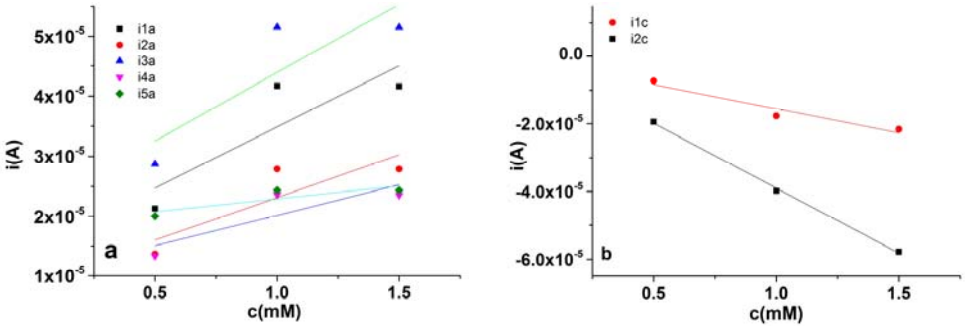

Fig. 6. Dependencies of the anodic (a) and cathodic (b) peak currents on concentration of **2** from DPV experiments

Equations of peak current dependencies on concentration *i(c)* for compound **2** are given in Fig. 6 and Table 4. It can be noticed that the slopes of concentration dependencies of the anodic peak currents are different: the values of the slopes are of about 20 $\mu A(mM)^{-1}$ for the first and the third peaks, and 10 $\mu A(mM)^{-1}$ for the second and fourth peaks; the fifth peak slope is about half the value of the fourth. For cathodic peaks the dependency of current on concentration is different, the second peak is obviously more prominent then the first one. These dependencies (Table 4) are useful from analytical point of view and can be used as calibration curves for the assessment of concentrations of **2,** using the DPV method.

In Table 4 are also given the equations of the dependencies of peak potential *vs* logarithm of concentration for anodic and cathodic processes. It is shown that the cathodic peaks are situated at constant potentials, while the anodic ones vary; with only 4mV/decade for a1, but with 48 mV/decade for a2, 43 mV/decade for a3, 77 mV/decade for a4, and 93 mV/decade for a5.

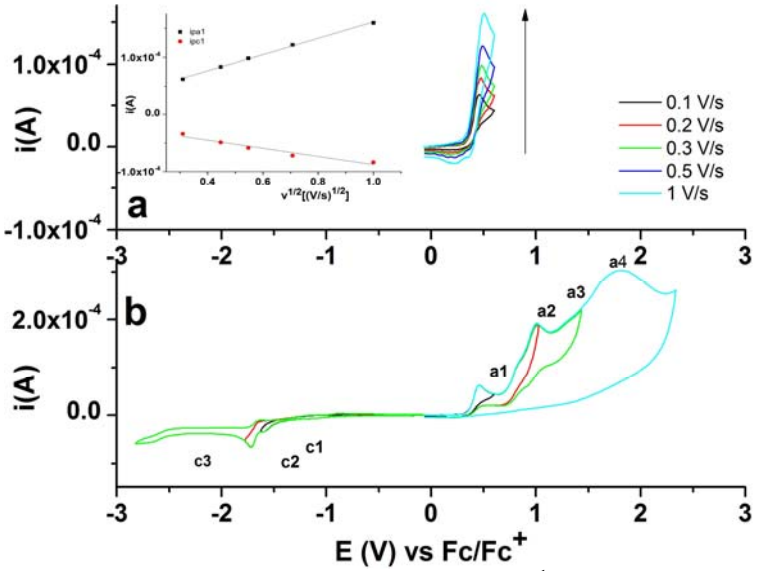

Fig. 7. CV curves at different scan rates: 0.1; 0.2; 0.3; 0.5; 1Vs^{-1} in the domains of the peaks c1 and a1, respectively, (a) and at various scan domains at 0.1 Vs^{-1} (b) for **2** (1.5 mM) in 0.1M TBAP, CH_3CN; (inset of (a) peak current dependency on square root of the scan rate)

The obtained peaks for **2** were assessed as summarized in Table 3, where the main oxidation and reduction processes are included, and the proposed oxidation mechanism was given in Scheme 2.

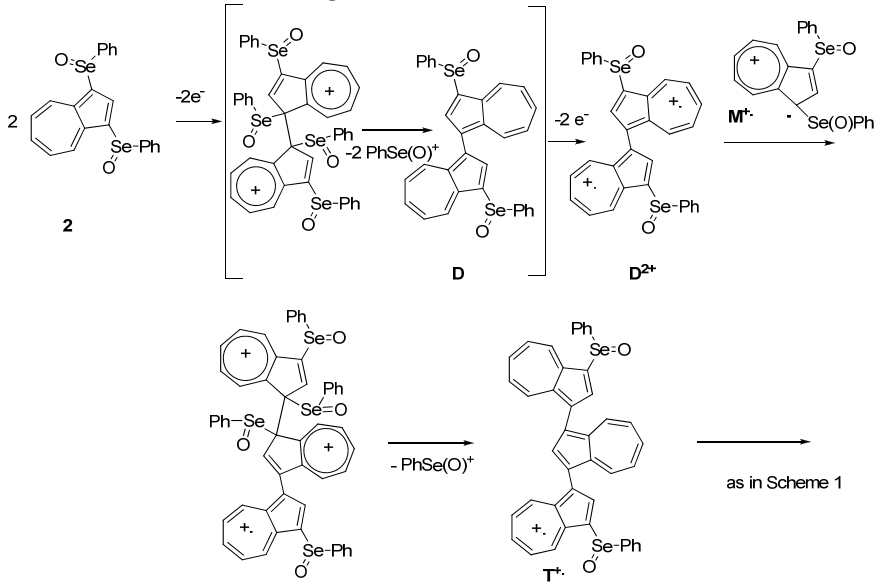

Scheme 2

Comparison between compounds 1 and 2

A comparison of **1** and **2** is given in Fig. 8. The shape of the DPV and CV curves of the disubstituted compound is similar to that of the monosubstituted one, due to the easy removal of the phenylseleninyl group. It is an expected behaviour, because the structures of the azulenic oligomers is common, as it can be seen in Scheme 2. However, the first oxidation potential is higher, and the first reduction potential is lower in absolute value, given the presence of two mild electron withdrawing groups [PhSe(O)]. It can be seen that the potentials of the reduction and oxidation peaks are shifted towards more positive values in comparison with those for **1**. For instance, the potentials of the peaks c1 for **1** and **2** are -1.67 V and -1.61 V, while those for the oxidation peaks a1 are 0.38 V and 0.39 V. The current intensity of the main peaks (a1, a2, a3, c1, c2) is almost double for the disubstituted azulene, while the other smaller peaks show generally higher values for **2**.

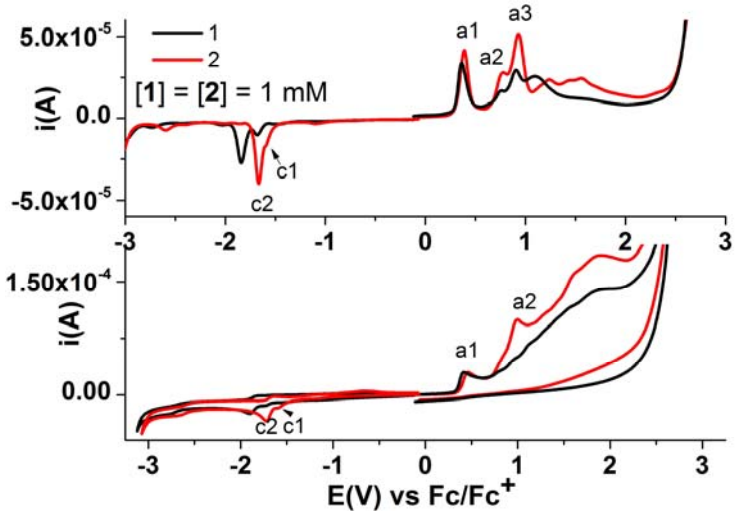

Fig 8. Comparison of DPV and CV for **1** (1 mM) and **2** (1mM) in 0.1 M TBAP, CH_3CN

Table 5

Values for potentials of the first oxidation (E_{a1}) and reduction (E_c) peaks for related selenium derivatives

Compound	E_{a1} (V)	E_c (V)		Reference
AzSePh	0.36	-1.82		[24]
AzSeOPh	0.37	-1.67	-1.84	Present work
$Az(SePh)_2$	0.38	-1.65		[24]
$Az(SeOPh)_2$	0.39	-1.61	-1.67	Present work

The values obtained for redox potentials (in V) of the two compounds studied in this paper are in agreement with those previously obtained in the study of unoxidized selenium derivatives [24], and with those for similar sulphur derivatives [20]: E_a: 0.35, E_c -1.90, -2.31 for Az(SPh) and E_a: 0.31, 0.55, 0.76, 1.03; E_c: -1.75, -2.33 for $Az(SPh)_2$. Thus, phenyl azulenyl selenides show oxidation and reduction potentials of about 10 mV more negative than the corresponding selenoxides (Table 5).

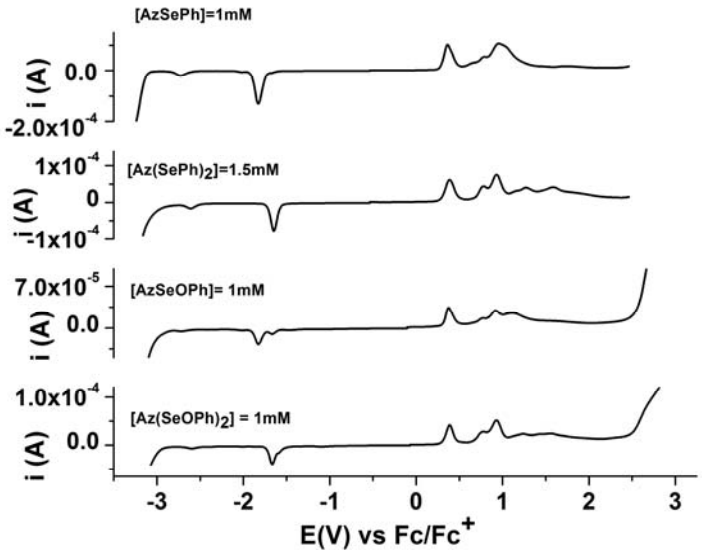

Fig 9. Comparison between the corresponding compounds from two classes of selenium compounds: selenides and selenoxides

Given the similar shape of the DPV curves (Fig. 9) for the two classes of compounds - selenides and selenoxides, it is clear that, in oxidations, the reactive part of the molecule is azulene, selenium redox chemistry being less involved. These systems, oxidized to cations, can also be stabilized through interactions with residual water from the solvent to azulenequinones, which decay to more stable structures such as phthalates.

The diffusion coefficients are also different for the mono and disubstituted azulenes ($D_1 = 1.08 \cdot 10^{-6}$ cm^2/s < $D_2 = 3.05 \cdot 10^{-6}$ cm^2/s). The higher diffusion coefficient has been obtained for the dimmer, and not for the monomer, which has the lowest mass (M_2 =470.2 g/mol > M_1= 299.2 g/mol). The obtained values could be rationalized either by the fact that the bis derivative **2** is more symmetrical than the mono derivative **1** (this lows the azulene polarizability), or by a different number of electrons involved in the first peak for **2** (n = 3 > 2), due to the higher oxidizable character of **2** (which can be oxidizable involving also selenium from

+4 to +6). For instance, in the last case, the calculation of D_2 with n = 3 leads to $D_2 = 0.9 \cdot 10^{-6}$ cm^2/s, value situated in the expected range of dependence.

4. Conclusions

The electrochemical behavior of azulene compounds containing selenium is influenced by the number of selenium groups and the oxidation state of selenium. The potentials of the anodic and cathodic peaks are shifted towards more positive values, and there is an increase of the peaks current intensities for the disubstituted azulenes, in comparison with the monosubstituted ones, in agreement with the number and effect of seleninyl substituents. The diffusion coefficients are different for the mono and disubstituted seleninyl azulenes.

REFERENCES

1. *A.C. Razus, L. Birzan, M. Cristea, E.A. Dragu, A. Hanganu*, Monatsh. Chem., **vol. 142**, pp. 1271, 2011.
2. *H.M. Priestly*, Brevet US 3642909, **1972**.
3. *S.J. Kuhn, J. C.Mcintyre,* Brevet US 3493586, **1970**.
4. *A. Schwarcz, G.D. Brindell*, Brevet US 3489744, **1970**.
5. *T.N. Srivastava, R.C. Srivastava, M. Srivastava*, Indian J. Chem. Section A, **vol. 21**, pp. 539, 1982.
6. *B.M. Phillips, L.F. Sancilio, E. Kurchacova*, J. Pharm. Pharmacol., vol. 19, no. 10, pp. 696, 1967.
7. *W.E. Rutzinski, T.M. Amiabhavi, N.S. Birdarar, C.S. Patil,* Inorg. Chim. Acta, **vol. 67**, pp. 177–182, 1982.
8. *I.D. Sadekov, I.A. Barchan, A.A. Maksimenko, et al*., Khim.-Farmats. Zh., **vol. 9**, pp. 1073, 1982.
9. *P. Silks, A. Louis*, Curr. Org. Chem., **vol. 10**, pp. 1891, 2006.
10. *V.A. Potapov, S.V. Amosova*, Russ. J. Org. Chem., **vol. 39**, no. 10, pp. 1373, 2003.
11. *M.R. Detty, M.E. Logan*, Adv. Phys. Org. Chem., **vol. 39**, pp. 79–145, 2004.
12. *J. Młochowski, M. Brząszcz, M. Giurg, J. Palus, H. Wójtowicz*, Eur. J. Org. Chem., **vol. 6**, pp. 4329, 2003.
13. *J.P. Marin, A. Schwartz*, Tetrahedron Lett., **vol. 20**, no. 35, pp. 3253, 1979.
14. *D.L. Klayman, H.H. Gunter* (Eds.), Organic Selenium Compounds: Their Chemistry and Biology, Wiley, New York, **1973**.
15. *G. Combs, O. Levander, J. Spallholtz, J. Oldfield*, Selenium in Biology and Medicine, AVI, Westport, CT, **1987**.
16. *B. Dakova, L. Lamberts, M. Evers, N. Dereu,* Electrochim. Acta, **vol. 36**, pp. 631, 1992.
17. *B. Dakova, L. Lamberts, M. Evers*, Electrochim. Acta, **vol. 39**, pp. 501, 1994.
18. *L. Engman, J. Persson, C. Anderson, M. Berglund*, J. Chem. Soc. Perkin Trans. 2, pp. 1309, **1992**.
19. *G. A. Inel, M. Soare, M. Bujduveanu, S. Varga, E.M. Ungureanu*, *L. Birzan,* U.P.B. Sci. Bull., Series B, **vol. 76**, pp. 3, 2014.
20. *T. Shoji, J. Higashi, S. Ito, K. Toyota, T. Asao, M. Yasunami, K. Fujimori, N. Morita*, Eur. J. Org. Chem., pp. 1242, **2008**.

21. *R. J. Waltman, J. Bargon*, Can. J. Chem., vol 64, pp. 76, 1986. *J. Bargon, S. Mohmand, R. J. Waltman,* Mol. Cryst. Liq. Cryst., **vol. 93**, pp. 279, 1983.
22. *S. Takekuma, Y. Matsubara, H. Yamamoto, T. Nozoe*, Bull. Chem. Soc. Jpn. **vol. 60**, pp. 3721, 1987.
23. *H. Wakabayashi, T. Kurihara, K. Shindo, M. Tsukada, P.-W. Yang, M. Yasunami, T. Nozoe,* J. Chin. Chem. Soc. **vol. 45**, pp. 391, 1998.
24. *A. C. Razus, L. Birzan, A. Hanganu, M. Cristea, C. Enache, E.-M. Ungureanu, M. L. Soare,* Monatsh. Chem. **vol. 145**, pp. 1999, 2014.